A 6-18 GHZ, HIGH DYNAMIC RANGE MMIC AMPLIFIER USING A FEEDFORWARD TECHNIQUE

V. Steel, D. Scott and S. Ludvik

Teledyne Monolithic Microwave
1274 Terra Bella Ave.
Mountain View, CA 94043

ABSTRACT

A novel feedforward linearization technique has been developed to increase dynamic range in a broadband, microwave amplifier module. Results are reported on a 6-18 GHz amplifier that demonstrates third order intercept improvement ≈7 dB and second order intercept improvement ≈20 dB.

INTRODUCTION

Phased array antenna systems have defined a need for high dynamic range amplifiers, ie. those with simultaneously low noise figure, low distortion, while maintaining low power dissipation. Traditionally, high dynamic range comes at the expense of high DC power consumption, due to the efficiency limitations of the amplifiers. The feedforward compensation technique provides a circuit approach that cancels distortion signals with only a moderate increase in DC power requirements. Successful implementation of this approach has been previously demonstrated at rf frequencies as well as over narrow frequency bandwidths (1,2,3). Extension to broadband, microwave frequencies has been limited by stringent component matching requirements. Recent availability of MMIC components and their inherently good phase/amplitude matching provides a new tool for applying the feedforward concept. This paper reports results on a 6-18 GHz amplifier that demonstrates significant third and second order intercept point improvement (TOI≈7 dB, SOI≈20 dB) using the feedforward approach.

THEORY

Ideal

The block diagram of the feedforward system is shown in Fig. 1. The input signal is sampled, then recombined 180° out of phase to cancel the signal entering the distortion amplifier from the main amplifier. This leaves only the distortion signals being amplified in the distortion amplifier. The output of the distortion amplifier is then recombined 180° out of phase with the output of the main amplifier to cancel the distortion in the overall module output signal.

A unique feature of the feedforward approach is that all spurious signals generated in the main amp are cancelled, including intermodulation products, harmonics, power supply modulation, as well as noise. Ideally then, the module noise figure is set by the distortion amplifier, not the main amplifier. This allows a power amplifier with good distortion performance to be used for the main amp without sacrificing noise figure. Also, since the distortion amp is not amplifying a large signal, it will produce negligible distortion and can thus be optimized for noise figure.

The feedforward technique differs from other linearization techniques in several ways:

1. All spurious signals are cancelled, not just third order. This is important for broadband systems.
2. Cancellation occurs over a large range of input power. Other methods generally operate over a narrow range.

Non-ideal

Ideal operation assumes perfect cancellation -- of the fundamental signal in Loop 1, and of the distortion signals in Loop 2. The cancellation requirements are such that amplitude and phase balance be maintained between both signal paths in Loop 1 and both paths of Loop 2. Figure 2

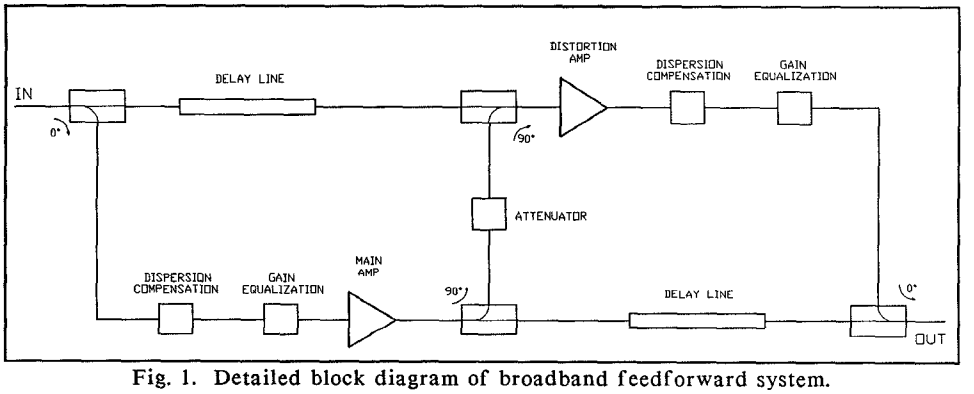

Fig. 1. Detailed block diagram of broadband feedforward system.

shows a simplified block diagram with the components labeled by their loss (or gain) in linear terms. The conditions for loop balance are summarized by the following vector equations:

Loop 1:

$$\frac{1}{\vec{S}_1\vec{L}_{D1}\vec{L}_C} = \frac{\vec{G}_1}{\vec{S}_2\vec{C}\vec{C}} \tag{1a}$$

$$\vec{G}_1 = \frac{\vec{C}\vec{C}\vec{S}_2}{\vec{S}_1\vec{L}_{D1}\vec{L}_C}, \tag{1b}$$

Loop 2:

$$\frac{\vec{G}_2}{\vec{C}\vec{C}\vec{U}_1} = \frac{1}{\vec{L}_C\vec{L}_{D2}\vec{U}_2} \tag{2a}$$

$$\vec{G}_2 = \frac{\vec{C}\vec{C}\vec{U}_1}{\vec{U}_2\vec{L}_{D2}\vec{L}_C}. \tag{2b}$$

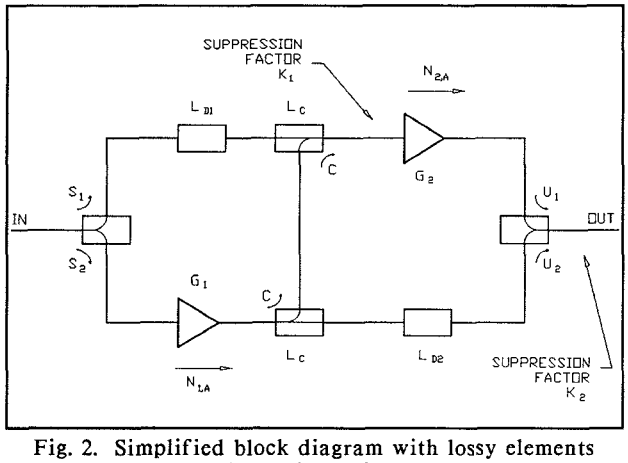

Fig. 2. Simplified block diagram with lossy elements lumped together.

Figure 3 shows the relationship between cancellation of a signal versus amplitude and phase imbalance.

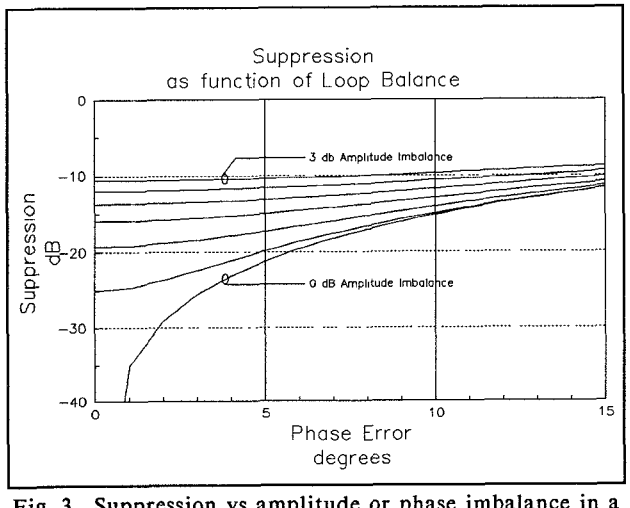

Fig. 3. Suppression vs amplitude or phase imbalance in a given loop.

The effect on the module performance of an imbalance in either Loop 1 or Loop 2 is discussed below:

Loop 1:

An imbalance in Loop 1 results in incomplete cancellation of the fundamental signal at the input to the distortion amplifier. This allows a portion of the input signal to be amplified by the distortion amplifier, resulting in partial cancellation of the desired output signal. If the fundamental cancellation is very poor at the input to Loop 2, then spurious signals may be generated within the distortion amplifier which can contribute to the overall output distortion.

Loop 2:

An imbalance in Loop 2 results in incomplete cancellation of the distortion products at the output. The most significant effect is on third and second order intercept point (TOI and SOI, respectively). The TOI is decreased by 1/2 of the degradation in distortion cancellation and the SOI is decreased by an amount equal to the degradation. In addition, the noise added from the main amp will not be fully cancelled, therefore contributing to overall noise figure.

Amplitude imbalance typically occurs as a result of amplifier ripple or coupler roll-off. This amplitude mismatch can be compensated by the use of gain equalizers and attenuators. These elements must be placed as in Fig. 1 to minimize the effect on noise figure or output losses.

Phase mismatch occurs as a result of dispersion, delay errors, and phase offset. One can delay match the two paths of each loop and provide compensating phase offset as necessary, but compensating for dispersion is more difficult. Two methods can be used:

1. Use a dispersion compensation network connected in cascade with the amplifier to linearize the phase characteristic of the amplifier. This allows the active path to track the relatively linear phase delay line.

   One such approach to the dispersion compensation network consists of a coupled line phase shift section as described by Schiffman (4). This type of network has a response shown in Fig. 4, where the frequency axis can be tailored to a particular band, and the coupling can be chosen to produce a given deviation from linear phase. The circuit was designed using Touchstone® and realized using cascaded 4 finger Lange couplers. A comparison of modeled and measured results is shown in Fig. 5.
2. Use a dispersive delay line which matches the dispersion characteristic of the amplifier. The net difference in phase is therefore constant. One method of forming this delay line is with a slow-wave helix structure. The delay is adjusted by the length of the helix, and the dispersion is controlled by varying the pitch and the barrel-to-coil spacing(5). Other methods include designing a microstrip coupled line section into the delay line; also, using a constant-k low pass structure.

Third and Second Order Intercept

Overall performance depends upon the distortion levels of the individual amplifiers as well as the suppression achieved. The following simple model helps to predict third order intercept of a feedforward amplifier:

A suppression factor, K_1 and K_2, for Loop 1 and Loop 2, respectively, is defined as follows:

$$\vec{K}_1 = \frac{\vec{G}_1}{\vec{S}_2\vec{C}\vec{C}} + \frac{1}{\vec{S}_1\vec{L}_D\vec{L}_C}, \tag{3a}$$

$$\vec{K}_2 = \frac{\vec{G}_2}{\vec{C}\vec{C}\vec{U}_1} + \frac{1}{\vec{L}_C\vec{L}_{D2}\vec{U}_2}, \tag{3b}$$

where K=0 for perfect cancellation.

In linear terms, TOI can be expressed as

$$TOI = \sqrt{\frac{P_o^3}{P_3}}. \tag{4}$$

Fundamental power output is

$$P_{o,T} = P_{in}\left|\frac{\vec{K}_1\vec{G}_2}{\vec{U}_1} + \frac{\vec{G}_1}{\vec{S}_2\vec{L}_C\vec{L}_{D2}\vec{U}_2}\right|. \tag{5}$$

The contributions to output intermodulation distortion from the main amp and the distortion amp, respectively, are:

$$P_{3,M} = \frac{\left(\frac{\vec{K}_2\vec{G}_1}{\vec{S}_2}P_{in}\right)^3}{TOI_M^2} \qquad P_{3,D} = \frac{(\vec{K}_1\vec{G}_2P_{in})^3}{\vec{U}_1 TOI_D^2} \tag{6}$$

$$P_{3,T} = \left(\frac{(\vec{K}_2\vec{G}_1)^3}{\vec{S}_2^3 TOI_M^2} + \frac{(\vec{K}_1\vec{G}_2)^3}{\vec{U}_1 TOI_D^2}\right)P_{in}^3 \tag{7}$$

where TOI_M and TOI_D are the measured TOI of the main and distortion amplifiers, respectively. The TOI at the output is then

$$TOI_T = \sqrt{\frac{P_o^3}{P_3}} = \sqrt{\frac{\left(\frac{\vec{K}_1\vec{G}_2}{\vec{U}_1} + \frac{\vec{G}_1}{\vec{S}_2\vec{L}_C\vec{L}_{D2}\vec{U}_2}\right)^3}{\left(\frac{(\vec{K}_2\vec{G}_1)^3}{\vec{S}_2^3 TOI_M^2} + \frac{(\vec{K}_1\vec{G}_2)^3}{\vec{U}_1 TOI_D^2}\right)}} \tag{8}$$

Similar analysis is used to determine the second order intercept, yielding

$$SOI_T = \frac{P_o^2}{P_2} = \frac{\left(\frac{\vec{K}_1\vec{G}_2}{\vec{U}_1} + \frac{\vec{G}_1}{\vec{S}_2\vec{L}_C\vec{L}_{D2}\vec{U}_2}\right)^2}{\left(\frac{(\vec{K}_2\vec{G}_1)^2}{\vec{S}_2^2 SOI_M} + \frac{(\vec{K}_1\vec{G}_2)^2}{\vec{U}_1 SOI_D}\right)}. \tag{9}$$

Note that as $K_1 \to 0$, TOI_D drops out, and only TOI_M affects the output. As $K_2 \to 0$, $TOI_T \to \infty$.

For small loop imbalances, TOI_T can be easily calculated by decreasing TOI_M by the amount of loss in the output path, and increasing it by 1/2 the suppression from Loop 2. Similarly, second order intercept is found by reducing SOI_M by the loss and increasing it by the full amount of suppression from Loop 2. This assumes no contribution from the distortion amp, which is valid under good Loop 1 cancellation conditions.

Noise Figure

To investigate the noise figure of a feedforward amplifier, the noise figure is expressed as:

$$F_T = \frac{S_{in}/N_{in}}{S_{out}/N_{out}} = \frac{S_{in}}{S_{out}}\left(\frac{N_{in}+N_A}{N_{in}}\right) \tag{10}$$

Signal and noise power is defined as follows:

$$S_{out} = \frac{S_{in}\vec{K}_1\vec{G}_2}{\vec{U}_1} + \frac{S_{in}\vec{G}_1}{\vec{S}_2\vec{L}_c\vec{L}_{D2}\vec{U}_2}$$

$$= S_{in}\left(\frac{\vec{K}_1\vec{G}_2\vec{S}_2\vec{L}_C\vec{L}_{D2}\vec{U}_2 + \vec{G}_1\vec{U}_1}{\vec{U}_1\vec{S}_2\vec{L}_C\vec{L}_{D2}\vec{U}_2}\right) \tag{11}$$

$$N_A = |\vec{K}_2|N_{1,A} + \frac{N_{2,A}}{U_1}. \tag{12}$$

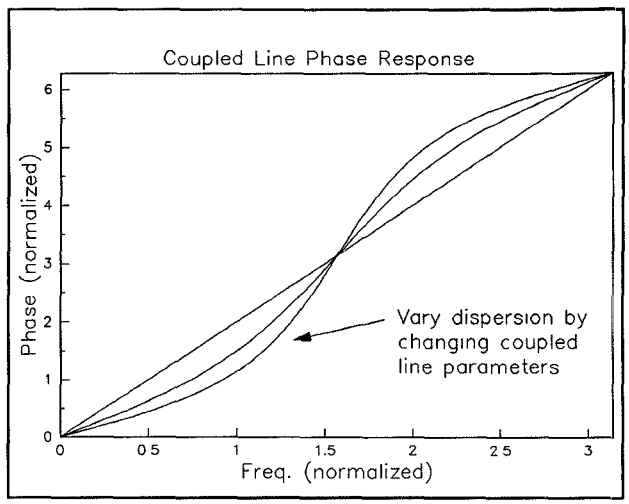

Fig. 4. Dispersion produced by Schiffman coupled line section.

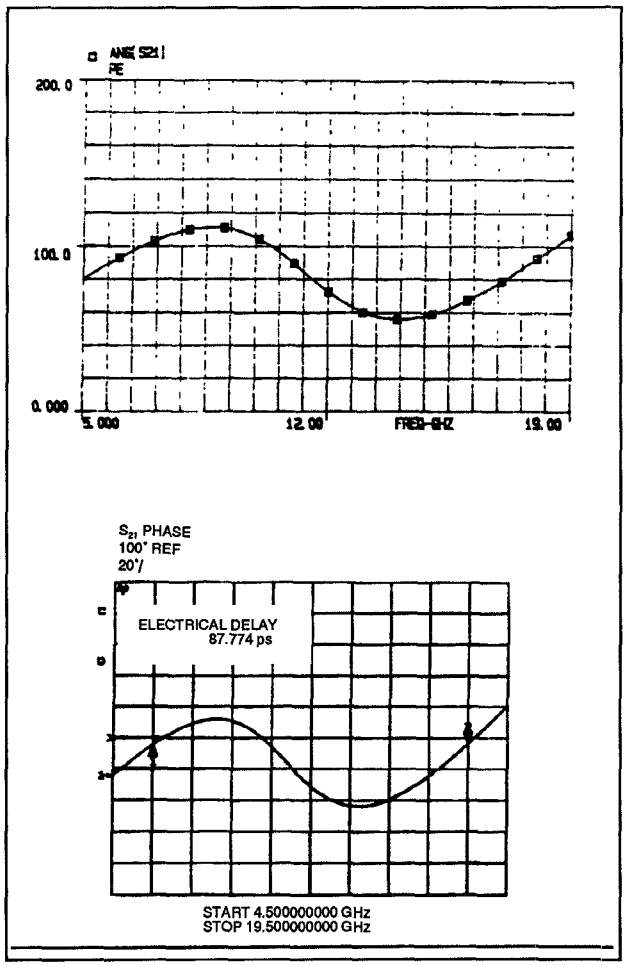

Fig. 5. Modeled vs measured dispersion curves.

Now the noise figure becomes:

$$F_T = \left| \frac{\vec{S}_2 \vec{L}_C \vec{L}_{D2} \vec{U}_2 \vec{U}_1}{\vec{K}_1 \vec{G}_2 \vec{S}_2 \vec{L}_C \vec{L}_{D2} \vec{U}_2 + \vec{G}_1 \vec{U}_1} \right| \left(\frac{N_{in} + |\vec{K}_2| N_{1,A} + \frac{N_{2,A}}{|\vec{U}_1|}}{N_{in}} \right). \quad (13)$$

Note that, in the ideal case, the suppression factors K_1 and $K_2 = 0$. Then,

$$F_T = \left| \frac{\vec{S}_2 \vec{L}_C \vec{L}_{D2} \vec{U}_2}{\vec{G}_1} \right| \left(1 + \frac{N_{2,A}}{N_{in} |\vec{U}_1|} \right).$$

which indicates the noise figure of the overall feedforward amplifier is affected by noise added from the distortion amp only.

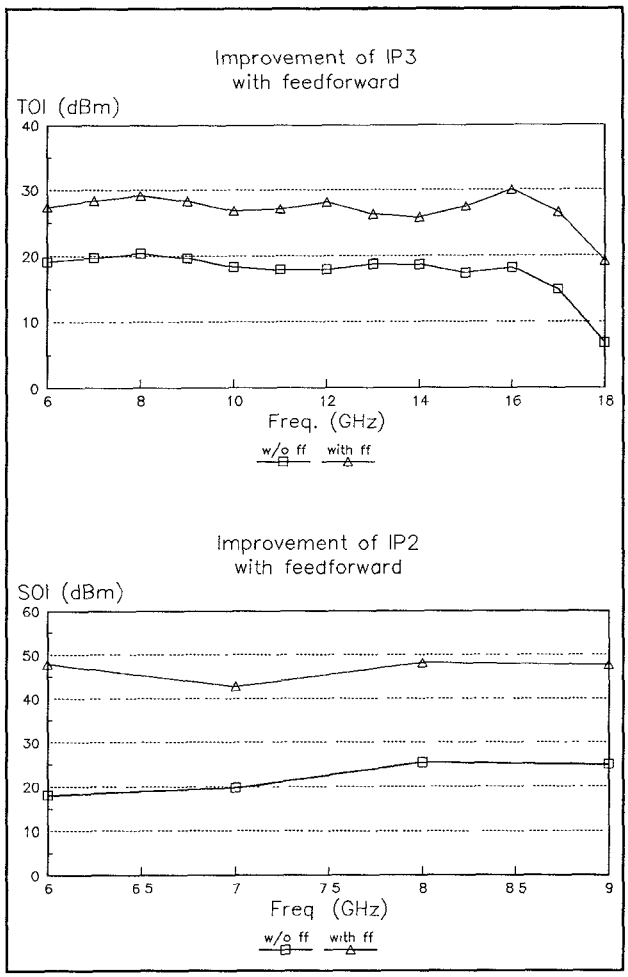

Fig. 6. Measured Third and Second order intercept point improvement with feedforward.

EXPERIMENTAL RESULTS

Experimental verification of broadband feedforward compensation was carried out using prototype amplifier operating in the 6-18 GHz band. The prototype used identical main and distortion amplifiers, each consisting of 3 cascaded TMM85001 MMIC distributed amplifiers. Discrete components were used to provide loop coupling and input/output combining. The delay path used variable delay lines, with a dispersion characteristic matching that of the amplifiers' to within 10°. The amplitude imbalance was not compensated, and was ±1.5 dB for both Loop 1 and Loop 2.

The third order intercept point (TOI) was first measured without the output from the distortion amplifier cancelling distortion signals, then measured with the distortion amplifier connected. As Fig. 6 shows, ≈7 dB of improvement in TOI and ≈20 dB of improvement in SOI is seen across the band. Amplitude equalization is possible to better than ±1/2 dB, which would improve cancellation further.

The noise figure of the individual components was measured and used to calculated the expected noise figure of the feedforward amplifier. Agreement between calculated and measured responses was within 1 dB.

CONCLUSION

Feedforward compensation has been demonstrated on a prototype 6-18 GHz amplifier to increase its second and third order intercept points. Measured performance improvement in both distortion and noise figure closely match theoretical predictions, with spurious signal cancellation of ≈15 dB being observed. These results indicate the potential in utilizing the feedforward concept in future microwave systems applications.

ACKNOWLEDGEMENTS

The authors would like to thank Tom Apel of Teledyne Monolithic Microwave for the dispersive phase shifter design. Gratitude is extended as well to Phil Lally of Teledyne MEC and Larry Wood of Teledyne Monolithic Microwave for discussions relating to helix slow-wave structures. Tan Phan is to be complemented for performing much of the required circuit testing.

REFERENCES

(1) J. Yamas, RF Design, July 1987, p. 50.
(2) H. Seidel et al., Bell System Technical Journal, May-June, 1968, p. 651.
(3) H. Seidel, Bell System Technical Journal, November, 1971, p. 2879.
(4) B. Schiffman, IRE Transactions on Microwave Theory and Techniques, April, 1958, p. 232.
(5) P. Lally, Personal Communication, Sept. 1989.